PCCP

Accepted Manuscript

This is an *Accepted Manuscript*, which has been through the Royal Society of Chemistry peer review process and has been accepted for publication.

Accepted Manuscripts are published online shortly after acceptance, before technical editing, formatting and proof reading. Using this free service, authors can make their results available to the community, in citable form, before we publish the edited article. We will replace this *Accepted Manuscript* with the edited and formatted *Advance Article* as soon as it is available.

You can find more information about *Accepted Manuscripts* in the Information for Authors.

Please note that technical editing may introduce minor changes to the text and/or graphics, which may alter content. The journal's standard Terms & Conditions and the Ethical guidelines still apply. In no event shall the Royal Society of Chemistry be held responsible for any errors or omissions in this *Accepted Manuscript* or any consequences arising from the use of any information it contains.

ROYAL SOCIETY OF CHEMISTRY

www.rsc.org/pccp

Cite this: DOI: 10.1039/c0xx00000x

www.rsc.org/xxxxxx

ARTICLE TYPE

Controlled Synthesis of Monodisperse α-Calcium Sulfate Hemihydrate Nanoellipsoids with a Porous Structure

Guangming Jiang,[a] Qiaoshan Chen,[a] Caiyun Jia,[a] Sen Zhang,[b] Zhongbiao Wu,[a] Baohong Guan[a,*]

Received (in XXX, XXX) Xth XXXXXXXXX 20XX, Accepted Xth XXXXXXXXX 20XX

DOI: 10.1039/b000000x

We report a facile and green chemical solution approach to synthesize monodisperse α-calcium sulfate hemihydrate (α-HH) nanoellipsoids with a length of 600 nm and a width of 300 nm by simply mixing Ca^{2+} and SO_4^{2-} glycerol-water precursor solutions in the presence of Na_2EDTA. The α-HH nanoellipsoid is formed through a Na_2EDTA-mediated self-assembly of small primary building blocks (α-HH domains: ~14 nm). The study on morphology evolution of α-HH reveals that controlled synergy of supersaturation (precursor concentration) and Na_2EDTA is crucial for the development of α-HH into nanoellipsoid. Further thermal annealing on the nanoellipsoid could make the α-HH domains transit into calcium sulfate anhydrites and grow up, generating the gaps between them and resulting in a porous structure. This work paves a new way to prepare high-quality α-HH with a monodisperse nanosize and a porous structure, promising their future application in many fields such as biomedicine.

Introduction

Fabricating inorganic materials with controllable morphology and hierarchical superstructure at nano and micro-scale is paramount for their optimized applications since the optical, electronic, magnetic, catalytic or biomedical properties are strongly morphology/structure-dependent.[1-4] α-calcium sulfate hemihydrate (α-HH), as an important class of highly cementitious biomaterials, has been extensively studied in chemical synthesis in hope to acquire specific morphology/structure for desired properties and applications.[5-8] For example, α-HH in the shape of hexagonal microprism with a low aspect ratio shows a high compressive/bending strength, which is in high priority to the construction materials and bone cements.[9-10] Micro-whiskers and wires of α-HH with a high aspect ratio have been used as a reinforcing agent in many polymer and ceramic composites due to the high thermal stability and compatibility with the polymer /ceramic matrices.[11-12] However, these kinds of α-HH are at microscale, making them unsuitable for many important applications, especially in biomedical field where the nano-size α-HH could be used as a smart and biocompatible drug carrier.

In this work, we report a facile and green chemical solution approach to synthesize high-quality α-HH nanoellipsoids with a uniform size and a hierarchical structure. The ellipsoid shape is preferable for use in bone cement and drug delivery due to the enhanced injectability to bone defects and transferability into cells.[13,14] Recently, our group has synthesized α-HH hexagonal nanoplates and nanospheres in the reverse micro-emulsion of water/CTAB/*n*-hexane/SDS.[15] Considering the high cost and complicated reaction system of micro-emulsion method, we keep our searching on a more facile and green solution chemistry to obtain well-defined α-HH nanoparticles. We found that simply mixing Ca^{2+} and SO_4^{2-} glycerol-water precursor solutions in the presence of Na_2EDTA could yield monodisperse α-HH nanoellipsoids with a length of ~600 nm and a width of ~300 nm. Different from the previously reported α-HH hexagonal nanoplate and nanospheres which are single crystalline nanoparticles, the α-HH nanoellipsoid is polycrystalline and formed by the self-assembly of small α-HH nanoparticle building blocks (α-HH domains).[16-19] Further annealing treatment on the as-synthesized α-HH nanoellipsoid could generate a porous structure. With the unique porous architecture and well-controlled nanosize/ morphology, the nanoellipsoid could be a promising drug carrier platform for future biomedical study.

Experimental Section

Materials

Analytic reagent grade glycerol (solvent), anhydrous $(NH_4)_2SO_4$, Na_2EDTA and $CaCl_2$ were all purchased from Sinopharm Chemical Reagent Co., Ltd., Shanghai, China.

Synthesis of the α-HH nanoellipsoid

In a typical procedure, two homogeneous precursor solutions of Ca^{2+} and SO_4^{2-} were prepared in two flasks before synthesis. The solution of SO_4^{2-} was composed of 10 ml H_2O, 250 ml glycerol and $(NH_4)_2SO_4$ (Solution I), while that of Ca^{2+} was prepared by dissolving $CaCl_2$ and Na_2EDTA into 50 ml glycerol (Solution II). Here the molar ratio of Ca^{2+} to SO_4^{2-} (Ca^{2+}/SO_4^{2-}) was fixed at 1.0. After both solutions were heated to and then kept at 90 ^oC for 20 min, the solution II was injected into the Solution I immediately. The mixed solution became turbid quickly or after a while, depending on the concentrations of Ca^{2+} or SO_4^{2-}. After reaction for 30 min, the solid products in the solution were separated by centrifugation (6000 rpm, 3 min), and further purified by

dispersing them into a mixture of water (10 ml) and acetone (30 ml) and centrifuged once more to remove glycerol and Na_2EDTA. After 3 times' wash, the products were dried at 60 °C for 3.0 h to remove the water and acetone. The dried powders were used for the characterization of composition and structure. In this work, different concentrations of Ca^{2+}, SO_4^{2-} and Na_2EDTA were employed to explore their effects on the α-HH morphology as well as the formation mechanism. It should be noted that all the given values of their concentration below refer to those in the mixed solution.

Characterization

The solid products were subjected to a powder X-ray diffraction analyzer (XRD, D/Max-2550 pc, Rigaku Inc., Tokyo, Japan), the thermogravimetry/differential scanning calorimetry analysis (TG/DSC, NETZSCH STA 409 Luxx, Selb/Bavaria, Germany) and Fourier transform infrared analysis (FTIR IRAffinity-1, Shimadzu, Japan) for the phase and composition identification. The XRD analysis was performed with Cu*K*a radiation at a scanning rate of 8 °/min in the 2θ range from 10 to 80°. For TG/DSC analysis, 20 mg of dry sample was sealed in an Al_2O_3 crucible with a lid and scanned at a rate of 10 °C min^{-1} under N_2 gas atmosphere. FTIR spectra were recorded on a pectrometer with a resolution of 4 cm^{-1} over the frequency range of 400-4000 cm^{-1}. The morphology evolution of the products was examined by the scanning electron microscopy (SEM, HITACHES-570, Hitachi, Tokyo, Japan). Transmission electron micrographs (TEM), the high angle annular dark-field scanning transmission electron micrographs (HAADF-STEM) and the selected area electron diffraction (SEAD) pattern were obtained on a transmission electron microscopy at an acceleration voltage of 200 kV (FEI TECNAI G2 F20 STWIN, USA).

Results and Discussion

Characterization of the calcium sulfate nanoellipsoids

Monodisperse calcium sulfate nanoellipsoids with a length of ~600 nm and a width of ~300 nm were obtained by simply mixing Ca^{2+} and SO_4^{2-} glycerol-water precursor solutions in the presence of 3.5 mM Na_2EDTA at 90 °C, as seen in Figure 1(a). SEM image of them under a low magnification is given in ESI. In our system, the medium is composed of only glycerol and water, which is much cleaner than the reported ones of concentrated electrolyte aqueous solutions or reverse microemulsions,[9,15] and is beneficial for calcium sulfate synthesis with superior purity and biocompatibility for medical application. Glycerol concentration in the medium is 98.44 mol%. On the basis of the thermodynamic phase-transition diagram of calcium sulfates in glycerol-water solution, a glycerol concentration of 98.44 mol % together with a temperature of 90 °C can ensure the α-HH to be the precipitated phase.[20] Figure 1(b) gives the XRD pattern of the as-synthesized nanoellipsoids, which exactly shows the principal peaks of α-HH (JSPDS card No. 041-0244). α-HH crystal is usually reported to be single-crystalline and displays a thermodynamically-favored prism or needle shape.[21] The ellipsoid is a new non-classic morphology/shape for α-HH. Though there are many reports on well-controlled synthesis of other calcium-based nanomaterials in a non-classic morphology, such as spherical $Ca_2(OH)PO_4$ and $CaCO_3$,[22-25] it is the first case for the calcium sulfate phase.

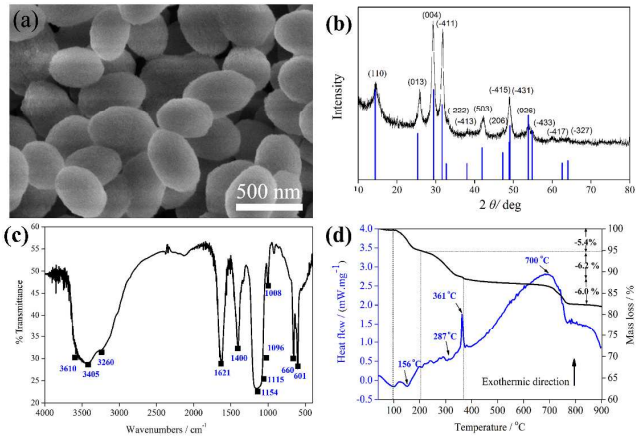

Figure 1. SEM (a), XRD pattern (b), FTIR pattern (c) and TG/DSC patterns (d) of the fresh α-HH nanoellipsoids synthesized in 98.44 mol% glycerol-water solution at 90 °C. (38 mM Ca^{2+} and SO_4^{2-}, 3.5 mM Na_2EDTA)

The FTIR spectrum in Figure 1(c) further confirms the α-HH phase by the evidence of its characteristic peaks emerging at 3260, 3405 and 3610 cm^{-1} (librational vibration of H_2O groups), 1008 cm^{-1} (v_1 SO_4^{2-} stretching), 1096, 1115 and 1154 cm^{-1} (v_3 SO_4^{2-} stretching), 601 and 660 cm^{-1} (v_4 SO_4^{2-} stretching).[26-27] Another two sharp peaks at 1400 and 1621 cm^{-1} assigned to COO^- stretching vibrations indicate the presence of the mediating agent Na_2EDTA in the ellipsoid. The TG/DSC curves of α-HH nanoellipsoids in Figure 1(d) show three weight-loss regions occurring at 25 - 200 °C (~5.4 wt%), 200 - 375 °C (~6.2 wt%) and 700 - 800 °C (~6.0 wt%) throughout the temperature range of 25 - 900 °C. The weight loss was minimized at temperatures higher than 800 °C. Correspondingly, three discrete phase transformation regions can be divided. Based on the endothermic peak at 156 °C on the DSC curve, the first weight loss refers to the elimination of crystal water of α-HH to form calcium sulfate anhydrite (AH, $CaSO_4$).[28] The lower crystal water content (5.4 wt%) than the theoretical one of α-HH (6.2 wt%) arises from the residue of Na_2EDTA. According to the endothermic peak at around 287 °C and the exothermic peak at 361 °C, the second weight-loss region (~6.2 wt%) is judged to be from the pyrolysis of Na_2EDTA, giving an amorphous phase (carbon and organic compounds). Subsequent elimination of this amorphous phase in the third step results in a weight loss of 6.0%, generating a large and broad exothermic peak at 700°C.[29] From the measured crystal water content, the purity of α-HH in the nanoellipsoid is calculated to be 87.1 wt% (5.4/6.2=87.1 wt%), which is consistent with the value (87.8 wt%) that is calculated by subtracting the content of Na_2EDTA [(100-6.2-6.0) wt% = 87.8 wt%]. This consistent proves that the nanoellipsoid is composed of only α-HH and Na_2EDTA. Figure 2a shows the HAADF-STEM image of one α-HH nanoellipsoid and the elemental mapping of Ca, S and N, indicating that the Ca (red), S (yellow) and N (brown) are homogeneously distributed on the surface of α-HH nanoellipsoid. Elements Ca and S belong to the α-HH, while the element N is from the Na_2EDTA, which proves that Na_2EDTA is adsorbed on the surface of α-HH. However, the color of N is not so dense as those of Ca and S, implying the low concentration of Na_2EDTA. All the above analysis indicate that the as-synthesized nanoellipsoids are mainly composed of α-HH

(87.8 wt%) with some Na_2EDTA on the surface.

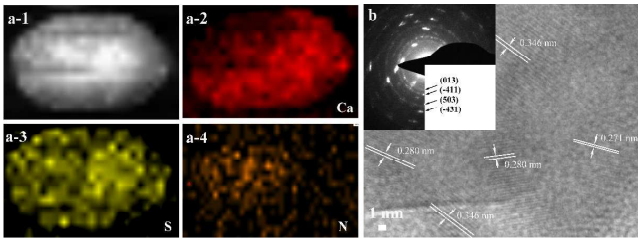

Figure 2. (a) HAADF-STEM image and surface elemental distribution analysis of the as-synthesized α-HH nanoellipsoid by elemental mapping of Ca (red), S (yellow) and N (brown). (b) HRTEM and SEAD (inset) images obtained from the area at the edge of the nanoellipsoid.

The non-classic morphology of α-HH nanoellipsoid displayed in Figure 1a and the obvious broadening of characteristic diffraction peaks compared to the standard peaks (in blue) on XRD pattern (Figure 1b) suggest that the nanoellipsoid should be polycrystalline. The domain size determined from the X-ray diffraction data with the Debye-Scherrer formula is about 14 nm (the calculation detail see ESI). Figure 2b shows a typical HRTEM image from the edge of the nanoellipsoid. The value of the lattice spacing of 0.280 and 0.346 nm measured by the HRTEM is consistent with that of (-411) and (013) interplane spacing of α-HH (JSPDS card No. 041-0244). The corresponding SEAD pattern in Figure 2b shows the diffraction rings and also some spots with random orientation, which overall confirms the polycrystalline nature of the α-HH nanoellipsoid. The values of the *d* spacing obtained from the diffraction ring are 0.346, 0.280 and 0.211 nm, corresponding to the (013), (-411) and (503) planes of α-HH.

To better understand the forming process of α-HH ellipsoid, morphology evolution of α-HH with reaction time was examined. The representative TEM images are presented in Figure 3. At the beginning of the process (sample collected immediately after mixing the precursor solutions), only very small calcium sulfate nanoparticles of 5 nm are obtained, as marked by the blue arrow in Figure 3a. After 5 min, the nanoprticles grow to a larger size. They start to assemble and some embryos of α-HH ellipsoid could be discerned, as seen in Figure 3b. After 10 min, the shape and profile of α-HH ellipsoid become clear (Figure 3c). However, there are still many nanoparticles around, which are believed to be the primary building blocks (primary α-HH domains). Thirty minutes later, the assembly process finishes, and no small nanoparticles could be found (The poor uniformity and smaller size here is believed to arise from the disturbance to the assembly process by the sample collecting). The α-HH nanoellipsoids look smaller than the original embryo, and the body appears denser with clear boundary (Figure 3d). Actually during this stage, the ellipsoid body also undergoes the Ostwald ripening process, constructing links between the small α-HH domains and increasing their crystallinity. The morphology evolution study of α-HH clearly demonstrates a Na_2EDTA-mediated self-assembly crystallization process for α-HH ellipsoid formation.

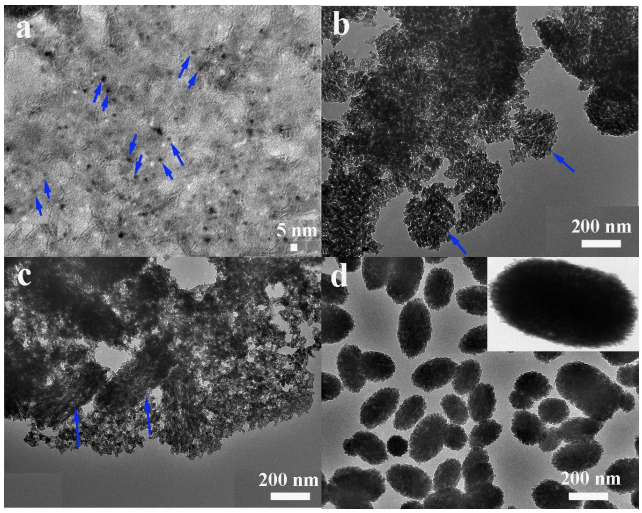

Figure 3. Morphology evolution of the α-HH nanoellipsoid (a) 0 min; (b) 5 min; (c) 10 min; (d) 30 min in 98.44 mol% glycerol-water solution at 90 °C . (38 mM Ca^{2+} and SO_4^{2-}, 3.5 mM Na_2EDTA)

Effects of reactant concentration on morphologic variation in the α-calcium sulfate hemihydrate

$CaCl_2$ and $(NH_4)_2SO_4$ serve as Ca^{2+} and SO_4^{2-} resources for α-HH synthesis. Figure 4 shows the morphology and size evolution of α-HH with increasing $CaCl_2$ and $(NH_4)_2SO_4$ concentration (Ca^{2+}/SO_4^{2-} = 1.0) from 25 to 50 mM under 3.5 mM Na_2EDTA at 90 °C. Under a low $CaCl_2$ concentration of 25 mM, the as-synthesized α-HH nanoparticle looks like a shuttle rather than an ellipsoid, with some flakes on the surface. The flake appears much smooth, compared to that of the particle body. In the gap of flakes, there are many tiny nanoparticles (~50 nm) building up the body of the ellipsoid. With increasing $CaCl_2$ concentration to 32 mM, perfect rod-like particles form with a length of 1000 nm and a width of 350 nm, and the flakes disappear. Most interestingly, a bundle of tiny rods of diameter 100 nm emerge at both ends of each particle. Similar phenomenon was reported in hydroxyapatite synthesis by using glutamic acid and aspartic acid as crystal templates. Imperfect oriented attachment and the stereospecific interaction between the mediating agent and the crystal surface steps, which affect the orientation of crystal growth, is believed to be the reason.[30]

With further increase in $CaCl_2$ concentration to 38 mM, monodisperse nanoellipsoids are obtained with a length of ~600 nm and a width of ~300 nm. The surfaces and ends appear very clean, and the aspect ratio decreases. When the $CaCl_2$ concentration is further raised to 44 mM, the ellipsoids turn to be smaller with a length of ~300 nm and a width of ~100 nm, but some aggregation occur and the surface become a little rough. Under 50 mM $CaCl_2$, the aggregation becomes much more severe, and no monodisperse particle could be collected.

The Zeta potential results in Figure 4f show that the α-HH nanoparticles are negatively charged, but the charge decreases with increasing $CaCl_2$ concentration. The negative surface charge should be from the COO- group of Na_2EDTA, which provides the electronic repulsive force among particles and prevents their aggregation. So besides as the mediating agent, Na_2EDTA serves as capping agent to stabilize the particles. The increased zeta potential suggests that there is less charge on the particles, which

reduces the stability of the particles. This is consistent with the more and more severe aggregation under higher $CaCl_2$ concentration.

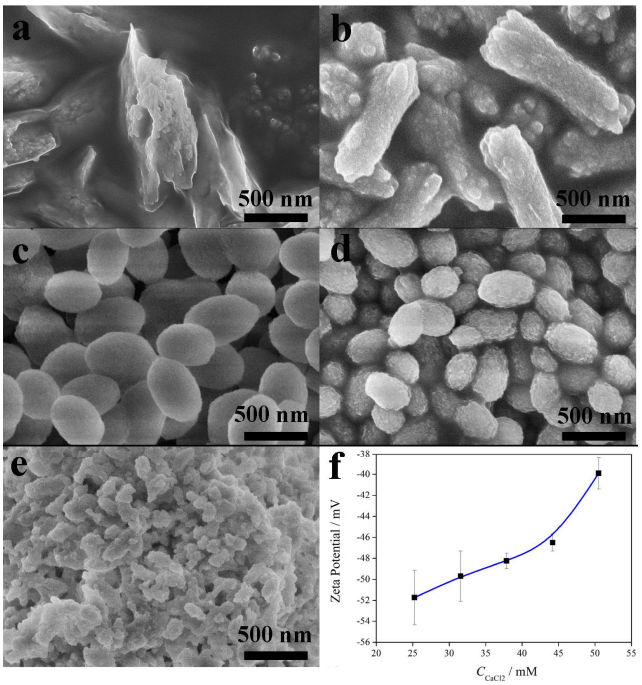

Figure 4. SEM images of the as-synthesized α-HH nanoellipsoid with increasing $CaCl_2$ concentration (Ca^{2+}/SO_4^{2-} = 1.0). (a) 25 mM, (b) 32 mM, (c) 38mM, (d) 44 mM, (e) 50 mM, and the corresponding Zeta potential (f) in 98.44 mol% glycerol-water solution at 90 °C. (Na_2EDTA: 3.5 mM)

The mediating agent-assistant self-assembly crystallization proceeds by nucleation (domain formation), mediated self-assembly of domains and the sequent crystal growth.[31-32] The supersaturation determines nucleation kinetics, as well as the size and number of primary building blocks (α-HH domains), while Na_2EDTA directs the self-assembly of α-HH domains and the crystal growth. At a low supersaturation, nucleation is slow and stops soon, few Ca^{2+} and SO_4^{2-} ions are consumed and most of them are left for crystal growth. In this case, crystal growth continues after self-assembly of α-HH domains and affects final morphology. Conversely, a high supersaturation leads to a quick nucleation, which triggers much more nuclei and consumes most of the lattice ions. Nucleation process dominates and crystal growth is suppressed, in this case the self-assembly process determines the final morphology. A fast nucleation will also reduce the size of α-HH domain and generate small nanoellipsoids. In our system, supersaturation (S) could be expressed as follows:

$$S = \frac{a_{Ca^{2+}} \cdot a_{SO_4^{2-}} \cdot a_{H_2O}^{0.5}}{a_{Ca^{2+},eq} \cdot a_{SO_4^{2-},eq} \cdot a_{H_2O,eq}^{0.5}} = \frac{m_{Ca^{2+}} \cdot \gamma_{Ca^{2+}} \cdot m_{SO_4^{2-}} \cdot \gamma_{SO_4^{2-}} \cdot a_{H_2O}^{0.5}}{m_{Ca^{2+},eq} \cdot \gamma_{Ca^{2+},eq} \cdot m_{SO_4^{2-},eq} \cdot \lambda_{Ca^{2+},eq} \cdot a_{H_2O,eq}^{0.5}} = \frac{m_{Ca^{2+}} \cdot m_{SO_4^{2-}}}{m_{Ca^{2+},eq} \cdot m_{SO_4^{2-},eq}}$$

where a, m and γ donate the activity, concentration and activity coefficient, and the subscript eq refers to equilibrium. The activity coefficients and water activity are eliminated in the equation (1) since they are mainly determined by the molar ratio of glycerol to water rather than the Ca^{2+} and SO_4^{2-} concentration.[33] Equation (1) indicates that supersaturation is determined by initial Ca^{2+} and SO_4^{2-} concentration, and a higher concentration constructs a larger supersaturation. From Figure 4(a-b) implies that the supersaturation of 25 or 32 mM Ca^{2+} and SO_4^{2-} is not high enough, and the nucleation is slow, which is also reflected by the longer period elapsed for the solution to be turbid after the mixing of the Ca^{2+} and SO_4^{2-} precursor solutions (About 8 and 3 min for 25 and 32 mM $CaCl_2$ respectively, but only ~10 s for 38 mM $CaCl_2$. See the ESI). At such a low supersaturation, Na_2EDTA-directed crystal growth dominates, leading to the formation of flakes in Figure 4a and the tiny rods in Figure 4b. As the concentration increases to 38 mM or high to 50 mM, the solution turns turbid as soon as the Ca^{2+} and SO_4^{2-} precursor solutions are mixed. The nucleation is suggested to be accelerated and thus the crystal growth is mostly hindered, resulting in a self-assembly-controlled morphology development. In this case, the development of flakes and tiny rods on the particles are inhibited, and clean nanoellipsoids are formed, as seen in Figure 4(c-d). However, the fast nucleation creates so many α-HH domains, which overloads the capability of the limited Na_2EDTA molecules to assemble and stabilize well, leading to a reduced monodispersity in Figure 4(d-e). Furthermore, it reduces the size of α-HH ellipsoids, as those seen from Figure 4c to 4d. Overall, supersaturation is suggested to control nucleation kinetics of α-HH and determine the respective impact factor of nucleation, self-assembly and crystal growth on the morphology evolution.

Effect of Na_2EDTA concentration on morphologic variation in the α-calcium sulfate hemihydrate

Na_2EDTA has been proposed above to mediate the α-HH domains assembly and modulate the crystal growth, as well as to serve as the capping agent to stabilize the α-HH nanoellipsoids. To further exploit the role of Na_2EDTA during the formation of α-HH ellipsoid, dependence of the α-HH morphology on the increasing concentration of Na_2EDTA from 0.0 to 14.0 mM were examined under 44 mM Ca^{2+} and SO_4^{2-} in 98.44 mol% glycerol-water solution at 90 °C. Without Na_2EDTA, irregular nanorods with a size of ~50 nm and a poor dispersity precipitate (Figure 5a), while in the presence of 3.5 mM Na2EDTA, α-HH nanoellipsoids form, as seen in Figure 5b. The α-HH ellipsoid has a size of ~150 nm in width and ~350 nm in length, which is much larger than the nanorods. The remarkable difference in the size and morphology of α-HH particles obtained with and without Na_2EDTA further confirms the important role of Na_2EDTA in the built-up of α-HH domains into superstructure nanoellipsoids.

A further increase in Na_2EDTA concentration to 7.0 mM help acquire larger monodisperse α-HH ellipsoids (Figure 5c) with higher monodispersity and cleaner surface, which could be ascribed to the increased number of Na_2EDTA molecules in the solution serving for α-HH domain assembly and stabilization, leading to the formation of α-HH with a well-organized superstructure. Interestingly, these α-HH nanoellipsoids show a much similar size to those in Figure 4c, which were obtained at a lower supersaturation of 38 mM Ca^{2+} and SO_4^{2-}, and a lower Na_2EDTA concentration of 3.5 mM. The similar size obtained under different supersaturations disobeys the fact that a higher supersaturation generates smaller α-HH. Considering the double dosage of Na_2EDTA (7.0 mM) for Figure 5c, we speculate that

the higher concentration of Na_2EDTA contributes to lowering the supersaturation of 44 mM Ca^{2+} and SO_4^{2-} close to the level of 38 mM Ca^{2+} and SO_4^{2-}.

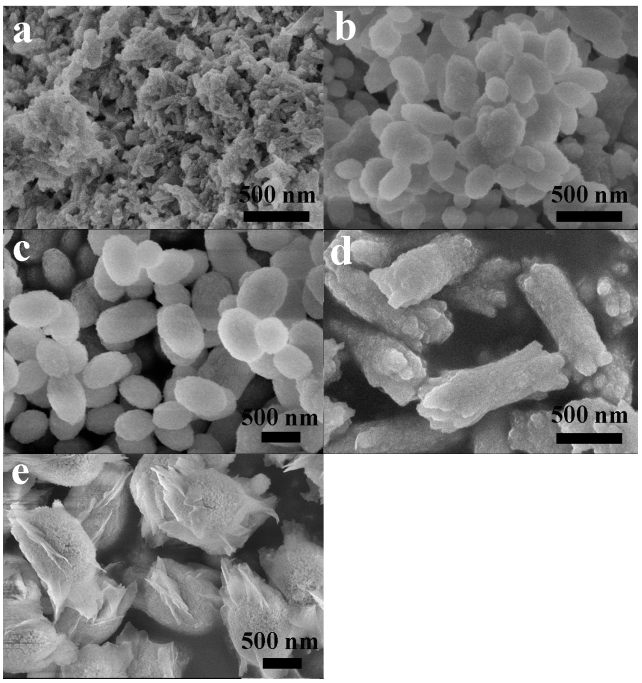

Figure 5. SEM images of the as-synthesized α-HH nanoellipsoid with increasing Na_2EDTA concentration (a) 0.0 mM, (b) 3.5 mM, (c) 7.0 mM, (d) 10.5 mM, (e) 14.0 mM in 98.44 mol% glycerol-water solution at 90 °C. (44 mM Ca^{2+} and SO_4^{2-})

The speculation is confirmed when the Na_2EDTA concentration is further increased. A Na_2EDTA concentration of 10.5 mM produces even larger α-HH nanorod ($l \times d$ =1000×350 nm, Figure 5d) with a similar morphology to those obtained under a lower supersaturation of 32 mM Ca^{2+} and SO_4^{2-} (Figure 5b). When the Na_2EDTA reaches 14.0 mM, the α-HH ellipsoid increases to 1200×900 nm (Figure 5e), and of particular interest is that some fish scale-like sheets growing on the surface, which looks like those obtained under a lower supersaturation of 25 mM Ca^{2+} and SO_4^{2-} (Figure 4a). All these results confirm that Na_2EDTA has the capability to lower the actual superaturation in solution and switch a nucleation-dominated crystallization process to a self-assembly-dominated process, and even to a crystal growth- dominated process. Actually, this capability could be partially ascribed to the well-known role of Na_2EDTA as a strong Ca^{2+} chelator.[34-35] A higher concentration of Na_2EDTA could chelate larger numbers of Ca^{2+}, restricting the release and reactivity of Ca^{2+} and thus lowering the supersaturation.[36-37]

Formation mechanism of the α-calcium sulfate hemihydrate nanoellipsoids

On the basis of above experimental evidence, a Na_2EDTA-mediated stepwise formation process of α-HH nanoellipsoid is described as Figure 6a. Initially, the Ca^{2+} and SO_4^{2-} nucleate into many α-HH domains, and Na_2EDTA mediates the assembly of α-HH domains into nanoellipsoid. Afterwards, a Na_2EDTA-directed crystal growth continues. During the assembly and crystal growth, the α-HH ellipsoids also undergo an Ostwald ripening process. The supersaturation (Ca^{2+} and SO_4^{2-} concentration) and Na_2EDTA concentration have a synergic effect in tuning the nucleation, assembly and crystal growth, generating different morphologies and sizes of α-HH particles, as schemed in Figure 6b, where the red particles are experimentally synthesized.

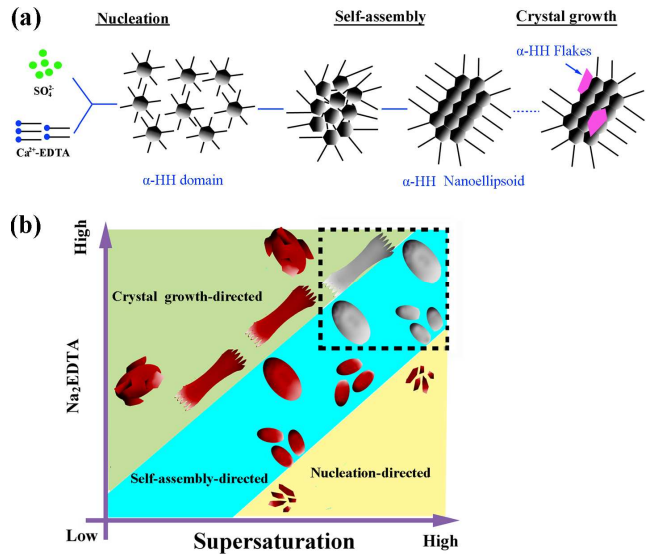

Figure 6. (a) Schematic illustration of the stepwise Na_2EDTA-mediated formation process of α-HH nanoellipsoid; (b) Schematic illustration of the synergic effect of supersaturation and Na_2EDTA concentration on morphology evolution of α-HH nanoparticles. (The red one is experimentally synthesized).

Three regions are divided by the product similarity, which are distinguished by colors. The yellow region is characterized by the high supersaturation and low Na_2EDTA concentration. In this region, a large supersaturation generates lots of α-HH domains and consumes most of the lattice ions, thus leaving few for crystal growth. At the same time, a low Na_2EDTA concentration provides less 'service' to orderly assemble and stabilize the numerous α-HH domains. Both lead to a nucleation-directed morphology development and the formation of many irregular rod-like α-HH particles with small size and poor dispersity. In the sky blue region, the mediating efficiency of Na_2EDTA is enhanced. It could chelate more Ca^{2+}, and restrict the release and reactivity of Ca^{2+}, lowering the actual supersaturation. At the same time, it helps the orderly assembly of the α-HH domains, suppressing their random morphology evolution. In this region, the morphology is determined by self-assembly, leading to the formation of monodisperse nanoellipsoid with clean surface. In the dark green region, the higher Na_2EDTA concentration alleviates the power of supersaturation, and the nucleation is suppressed. Crystal growth after the self-assembly determines the morphology of α-HH particle. Na_2EDTA directs the orientation of crystal growth through selective adsorption on crystal surfaces, leading to the formation of tiny rods and fish scale-like sheets on the surface of α-HH ellipsoid.

For nanoparticle synthesis using ions as reactants, the yield is usually the problem, since a high yield needs a higher reactant concentration, which produces a higher supersaturation and then results in an uncontrolled crystallization process. For example in our system, a higher concentration of Ca^{2+} and SO_4^{2-} worsens the particle monodispersity, limiting the scale-up production of α-HH nanoellipsoid. However, the capability of Na_2EDTA to lower the

actual supersaturation provides the possibility to synthesize monodisperse α-HH nanoellipsoid at an even high supersaturation, as predicted by the grey nanoellpsoid on the right top of blue sky region in Figure 6b. This is quite beneficial to develop our method for the industrial production of monodisperse α-HH nanoellipsoid.

Generation of the porous structure

The as-synthesized α-HH nanoellipsoids were treated by thermal annealing at 300, 450 and 600 ^{o}C under air flow for one hour, respectively. Interestingly, the α-HH nanoellipsoids annealed at 300 and 450 ^{o}C keep the shape but some pores emerges as seen in Figure 7b and 7c, while at 600 ^{o}C lose the shape and disintegrate into smaller particles with a size of 100 - 200 nm, as seen in Figure 7d. It seems that the α-HH domains transform to AH domains above 300 ^{o}C, which grow into larger size at high temperatures, leading to the gap generation between the domains and then the pore formation. Such strategy is also utilized to prepare porous Fe_3O_4 from polycrystalline Fe_3O_4 through high temperature treatment.[38] The annealing temperature here is set to make sure no Na_2EDTA is decomposed, ruling out the possibility of pore formation from the decomposition of Na_2EDTA. The domains show a growing size from ~100 to ~150 nm with increasing temperature from 300 to 450 ^{o}C, which could be ascribed to the accelerated growth rate of domain at a higher temperature. Due to the grown domain size, an increase in the pore size and an obvious boundary between domains are observed from Figure 7a to 7c. However, an even higher temperature of 600 ^{o}C makes the domain too large and breaks the ellipsoid down into individual $CaSO_4$ crystals.

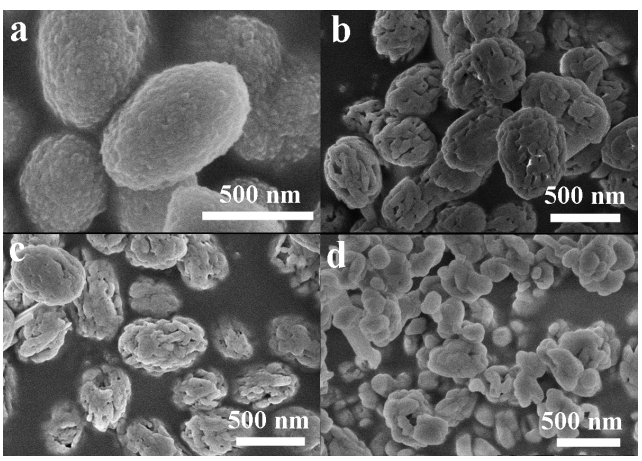

Figure 7. SEM images of the as-synthesized α-HH nanoellipsoid (a), and those after one hour's annealing at 300 ^{o}C (b), 450 ^{o}C (c) and 600 ^{o}C (d) under the air flow.

The specific surface area of the as-synthesized α-HH nanoellipsoids (Figure 7a) and the porous nanoellipsoids (Figure 7c) are compared by conducting the nitrogen adsorption-desorption isotherm analysis, and the results are shown in ESI. The porous nanoellipsoid is suggested to show a 10 times larger specific surface area (37.9 cm^3g^{-1}) than the as-synthesized α-HH nanoellipsoid (3.8 cm^3g^{-1}). The average pore size is calculated to be 38 nm by the Barrett-Joyner-Halendan method from the adsorption branch. This porous structure is ideal for drug storage. Considering the excellent biocompatibility and biodegradability, the porous nanoellipsoid should be a promising carrier for drug delivery. Through controlling the annealing time and temperature, a good control in the pore size, volume and shape could be achieved and more work on biomedical study is undergoing.

Conclusions

This work presents a robust wet-chemistry to synthesize monodisperse α-HH nanoellipsoids by simply mixing Ca^{2+} and SO_4^{2-} glycerol-water precursor solutions in the presence of Na_2EDTA. The α-HH nanoellipsoid is produced by the Na_2EDTA-mediated self-assembly of small α-HH nanoparticle building blocks. Controlled synergy of supersaturation and Na_2EDTA is crucial for the development of α-HH into nanoellipsoid. Supersaturation controls the nucleation kinetics and determine the respective impact factor of nucleation, self-assembly and crystal growth on the morphology evolution, while Na_2EDTA restricts the supersaturaton through chelating the Ca^{2+} and simultaneously mediates the self-assembly of α-HH domains and the crystal growth. Na_2EDTA also serves as capping agent to stabilize the α-HH nanoellipsoids. When subjected to thermal annealing, the α-HH nanoellipsoid could transform into a porous structure. The unique size, morphology and porous architecture make the nanoellipsoid a potential platform for drug delivery in the future biomedical application.

Notes and references

[a] *Department of Environmental Engineering, Zhejiang University, Hangzhou 310058, China. Fax: 86-571-88982026; Tel: 86-571-88982026; E-mail:guanbaohong@zju.edu.cn*
[b] *Department of Chemistry, University of Pennsylvania, Philadelphia, Pennsylvania 19104, USA.*

† Electronic Supplementary Information (ESI) available: See DOI: 0.1039/b000000x/

[1] Peng, X. G.; Manna, L.; Yang, W. D.; Wickham, J.; Scher, E.; Kadavanich, A.; Alivisatos, A. P. *Nature* 2000, **404**, 59-61.
[2] Shieh, F. K.; Wang, S. C.; Leo, S. Y.; Wu, K. C. *Chem.-Eur. J.* 2013, **19**, 11139-11142.
[3] Zhang, S.; Jiang, G.; Filsinger, G. T.; Wu, L.; Zhu, H.; Lee, J.; Wu, Z.; Sun, S. *Nanoscale* 2014, **6 (9)**, 4852-4856.
[4] Wang, L.; Liu, C. H.; Nemoto, Y.; Fukata, N.; Wu, K. C. W.; Yamauchi, Y. *RSC Adv.* 2012, **2**, 4608-4611.
[5] Luo, K. B.; Li, C. M.; Xiang, L.; Li, H. P.; Ning, P. *Particuology* 2010, **8**, 240-244.
[6] Li, Z.B.; Demopoulos, G.P. *Ind. Eng. Chem. Res.* 2006, 45, 4517-4524.
[7] Jiang, W. G.; Pan, H. H.; Tao, J. H.; Xu, X. R.; Tang, R. K. Langmuir 2007, 23, 5070-5076.
[8] Jung, H. M.; Song, G. A.; Lee, Y. K.; Baek, J. H.; Ryoo, H. M.;Kim, G. S.; Choung, P. H.; Woo, K. M. *Biomater.* 2010, **31**, 29-37.
[9] Feldmann, T.; Demopoulos, G. P. *J. Cryst. Growth* 2012, **351**, 9-18.
[10] Wang, P.; Lee, E. J.; Park, C. S.; Yoon, B. H.; Shin, D. S.; Kim, H. E.; Koh, Y. H.; Park, S. H. *J. Am. Ceram. Soc.* 2008, **91(6)**, 2039-2042.
[11] Xu, A.; Li, H.; Luo, K.; Xiang, L. *Res. Chem. Intermed.* 2011, **37**, 449-455.
[12] Hou, S. C.; Wang, J.; Wang, X. X.; Chen, H. Y.; Xiang, L. Langmuir 2014, 30, 9804-9810.
[13] Zhang, L.; Gu, F. X.; Chan, J. M.; Wang, A. Z.; Langer, R. S.; Farokhzad, O. C. *Clin. Pharmacol. Ther.* 2008, **83**, 761−769.
[14] Chithrani, B. D.; Ghazani, A. A.; Chan, W. C. W. *Nano Lett.* 2006, **6**, 662-668.
[15] Kong, B.; Guan, B. H.; Yates, M. Z.; Wu, Z. B. *Langmuir* 2012, **28**, 14137-14142.

[16] Liu, Y.; Cui, Y. J.; Mao, H. Y.; Guo, R. *Cryst. Growth. Des.* 2012, 12, 4720 - 4726.
[17] Zhang, T. K.; Zhu, J. H.; Yao, H. B.; Yu, S. H. *Cryst. Growth Des.* 2007, **7 (12)**, 2419-2428.
[18] Yu, S. H.; Colfen, H.; Xu, A. W.; Dong, W. F. *Cryst. Growth Des.* 2004, **4 (1)**, 33-37.
[19] Fan, L.; Guo, R. *Cryst. Growth Des.* 2009, **9 (4)**, 1677-1682.
[20] Guan, B. H.; Jiang, G. M.; Fu, H. L.; Yang, L.; Wu, Z. B. *Ind. Eng. Chem. Res.* 2011, **50 (23)**, 13561-13567.
[21] Ling, Y. B.; Demopoulos, G. P. *Ind. Eng. Chem. Res.* 2005, **44(4)**, 715 – 724.
[22] Xu, A. W.; Antonietti, M.; Colfen, H.; Fang, Y. P. *Adv. Funct. Mater.* 2006, **16 (7)**, 903-908.
[23] Kim, S. J.; Park, C. B. Langmuir. 2010, 26 (18), 14730-14736.
[24] Liu, L.; Jiang, J.; Yu, S. H. *Cryst. Growth Des.* 2014, **14**, 6048-6056.
[25] Rees, G. D.; Gowing, R. E.; Hammond, S. J.; Robinson, B. H. *Langmuir*, 1999, **15(6)**, 1993 -2002.
[26] Prasad, P. S. R.; Chaianya, V. K.; Prasad, K. S.; Rao, D. N. *Am. Mineral.* 2005, **90**, 672-678.
[27] Mandal, P. K.; Mandal, T. K. *Cem. Concr. Res.* 2002, **32**, 313-316.
[28] Guan, B. H.; Jiang, G. M.; Wu, Z. B.; Mao, J. W.; Kong, B. *J. Am. Ceram. Soc.* 2011, **94 (10)**, 3261-3266.
[29] Li, W.; Lee, J. *J. Phys. Chem. C* 2008, **112**, 11679-11684.
[30] Wu, Y. J.; Tsai, T. W. T.; Chan, J. C. C. *Cryst. Growth Des.* 2012, **12**, 547−549.
[31] Guo, X. H.; Yu, S. H.; Cai, G. B. *Angew. Chem. Int. Edit.* 2006, **45 (24)**, 3977-3981.
[32] Adhikari, R.; Gyawali, G.; Kim, T. H.; Sekino, T.; Lee, S .W. *J. Environ. Chem. Eng.* 2014, **3(2)**, 1365-1370.
[33] Jiang, G. M.; Fu, H. L.; Savino, K.; Qian, J. J.; Wu, Z. H.; Guan, B. H. *Cryst. Growth Des.* 2013, **13 (11)**, 5128-5134.
[34] Yi, T.; Gao, S.; Li, B. *Polyhedron*, 1998, **17**, 2243-2248.
[35] Simpson, D. R. *Am. Mineral.* 1968, **53**, 432-444.
[36] Haders, D. J.; Burukhin, A.; Zlotnikov, E.; Riman, R. E. *Chem. Mater.* 2008, **20**, 7177-7187.
[37] Xie, R. Q.; Feng, Z. D.; Li, S. W.; Xu, B. B. *Cryst. Growth Des.* 2011, **11**, 5206-5214.
[38] Cheng, K.; Peng, S.; Xu, C. J.; Sun, S. H. *J. Am. Chem. Soc.* 2009, **131**, 10637-10644.